Modeling of Sugar Crystallization through Knowledge Integration

By *Petia Georgieva*, *Sebastião Feyo de Azevedo**, *Maria Joao Goncalves* and *Peter Ho*

This paper reports on the comparison of three modeling approaches that were applied to a fed batch evaporative sugar crystallization process. They are termed white box, black box, and grey box modeling strategies, which reflects the level of physical transparency and understanding of the model. White box models represent the traditional modeling approach, based on modeling by first principles. The black box models rely on recorded process data and knowledge collected during the normal process operation. Among various tools in this group artificial neural networks (ANN) approach is adopted in this paper. The grey box model is obtained from a combination of first principles modeling, based on mass, energy and population balances, with an ANN to approximate three kinetic parameters – crystal growth rate, nucleation rate and the agglomeration kernel. The results have shown that the hybrid modeling approach outperformed the other aforementioned modeling strategies.

1 Introduction

Development of a suitable process simulation model is an important engineering task, which can be used prior to conducting industrial experiments. Improving a process model will reduce not only the costs, but also the time that is normally required to optimise a process. There are three different modeling strategies that can be applied to develop a model, based on the nature of the information available. They can be classified as either first principles (known also as a white box), data-based (black box) or hybrid (grey box) approaches [1].

In this paper, these three modeling strategies are applied, in the context of an industrial sugar crystallization process, in order to examine if an improved process model can be achieved by adopting a hybrid modeling strategy instead of models based solely on white box or black box approaches. The search for efficient methods for process modeling is linked not only to the scientific interest of understanding fundamental mechanisms of crystallization, but also to the practical interest of production requirements. Nucleation, growth and agglomeration are three mechanisms that occur during sugar crystallization, which are known to be affected by several undefined operating conditions. This process will be briefly described in section 2.

Section 3 examines the first principles model of a sugar crystallization process. Although, this model accurately represent the behaviour of the process dynamics, crystal size distribution (CSD), quantified by the mean value (MA) and the coefficient of variation (CV) of the mass size distribution function is poorly predicted. This discrepancy is due to a lack of sufficient accuracy in modeling kinetic phenomena, such as crystal nucleation rate, growth rate and, in particularly, the effect of agglomeration. Although, the process variables that affect the kinetic mechanisms are rather well known, their nonlinear effect on the kinetic parameters makes the modeling difficult. However, a variety of empirical models have been proposed [2,3].

The second modeling alternative is data-based models, which rely only on data and knowledge collected during normal process operation and specially designed experiments. Artificial Neural Networks (ANN) and expert systems are the main tools belonging to this modeling approach. These models are comparatively easy to formulate, as long as enough and reliable process data can be collected. However, their main disadvantage is a lack a physical understanding and poor extrapolative properties of these models. Section 4 describes the design of an ANN model of the crystallization process. The third modeling approach, known as Knowledge-Based Hybrid Modeling (KBHM), is a combination of the first principles and data-based modelling, which aims at exploiting all sources of *a prior* knowledge/information about the process and incorporating it in the process model.

Knowledge integration follows the modular principle, which consists of the division of the process in several modules according to the kind of knowledge available in different parts of that process. This can be represented as a diagram of interconnected modules, where each model is expressed by an input-output relationship that is based on a particular modeling technique. There are two main KBHM architectures, complementary (serial) and competitive (parallel). In the parallel structure, different forms of knowledge about the same (sub)system is available for possible use. Modules compete for the right to represent the same part of the process (parameters, outputs, etc.). In the serial structure, different kinds of knowledge complement themselves. Usually, for known physical constraints (e.g. mass and energy balances) the most reliable models are still the mechanistic models, whereas data-based models are more efficient in modeling poorly defined parts of a process.

The knowledge-based hybrid (KBH) model described in section 5 takes advantage of the prior physical knowledge

[*] Dr. P. Georgieva (pgeorgieva@hotmail.com), Department of Chemical Engineering, Faculty of Engineering, University of Porto, R. Dr. Roberto Frias, 4200-465 Porto, Portugal; Prof. S. Feyo de Azevedo (corresponding author, sfeyo@fe.up.pt), Department of Chemical Engineering, Faculty of Engineering, University of Porto, R. Dr. Roberto Frias, 4200-465 Porto, Portugal; Dr. M. J. Goncalves, Department of Chemical Engineering, Polytechnic Institute of Porto, Av. António Bernardino de Almeida, 431, 4200-072 Porto, Portugal; Dr. P. Ho (peter@estg.ipvc.pt), Departamento de Ciências de Engenharia e Tecnologia, Escola Superior de Tecnologia e Gestão, Instituto Politécnico de Viana do Castelo, Av. Do Atlântico, apartado 574, 4900 Viana do Castelo, Portugal.

  1618-0240/03/0303-001 $ 17.50+.50/0

formulated by the mass, energy and population balances, while employing an ANN to model kinetic parameters. The motivation for the use of a neural network structure is based on the fact that it is a promising modeling tool, when theoretical knowledge is insufficient but experimental data is available, as it is the case here.

Finally, the ability to predict the process outputs (temperature of the massecuite and the brix of the solution) by these three models are evaluated in section 6. The most important achievement of this paper is an improvement in the reliability of the predicted CSD by the KBH model. An analysis of variance (ANOVA) and Tukey';s honestly significant difference tests were conducted which confirmed that better predictions were essentially obtained, in particularly for CV, by the hybrid model.

2 Sugar Crystallization Process Description

The industrial batch crystallizer is schematically represented in Fig. 1. It is carried out in a traditional pan with 'fixed' calandria, equipped with a total condensing steam valve and a

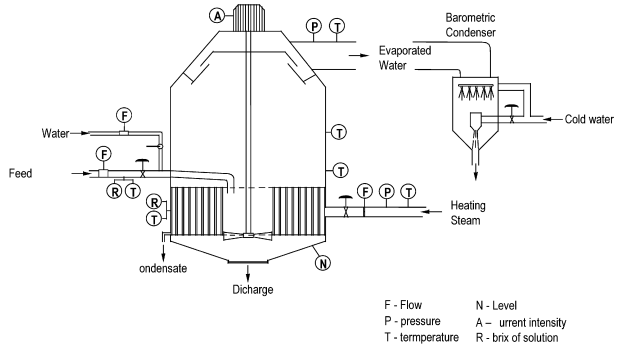

Figure 1. Industrial setup for a batch sugar crystallizer.

propeller stirrer. The batch cycle is divided in several phases. During the first phase the pan is partially filled with a juice containing dissolved sucrose (termed liquor). The liquor is concentrated by evaporation, under vacuum, until the supersaturation reaches a predefined value. At this point seed crystals are introduced into the pan to induce the production of crystals (crystallization phase). As evaporation takes place, further liquor or water is added to the pan. This maintains the level of supersaturation and increases the volume contents. Near to the end of this phase, the liquor is replaced by other juice of lower purity (termed syrup). The third phase consists of tightening which is controlled by the evaporation capacity.

The industrial unit is equipped with 15 sensors and the online collected measurements are summarised in Tabs. 1 and 2. Data from 15 batches were collected for a period of 4 months.

3 First Principles Model (White Box Model)

The first principles model considered below was investigated by several authors [4,5] and proved to give a relevant interpretation to the physical nature of the process considered. It consists of three parts.

Table 1. Measured variable data.

Notation	Process variable
F_f	Liquor/syrup feed flowrate
B_f	Feed Brix
T_f	Temperature of feed
F_w	Water feed flowrate
F_s	Steam flowrate
T_s	Steam temperature
P_s	Steam pressure
I_{agit}	Intensity of stirrer current
P_{vac}	Vacuum pressure
T_{vac}	Vacuum temperature
B_{sol}	Brix of solution
T_m	Temperature of solution
L	Level in the pan

Table 2. Constant operational and control variables.

Notation	Process variable
T_w	Temperature of feed water
Pur_f	Purity of liquor/syrup
t_{syr}	Initial time for introducing syrup
t_{seed}	Initial time of seeding

Mass Balances

Mass of water M_W, mass of impurities M_i, mass of dissolved sucrose M_s and mass of crystals M_c are included in the following set of differential equations[1)]

$$\frac{dM_w}{dt} = F_f \rho_f (1 - B_f) + F_w \rho_w - J_{vap} \tag{1.1}$$

$$\frac{dM_i}{dt} = F_f \rho_f B_f (1 - Pur_f) \tag{1.2}$$

$$\frac{dM_s}{dt} = F_f \rho_f B_f Pur_f - J_{cris} \tag{1.3}$$

$$\frac{dM_c}{dt} = J_{cris} \tag{1.4}$$

The heat input and the evaporation rate are given by the following correlations

$$Q = \alpha_s F_s \Delta H_s \tag{2}$$

$$J_{vap} = \frac{W+Q}{\lambda_{w(vac)}} + k_{vap}(T_m - T_{w(vac)} - BPE) \tag{3}$$

[1)] List of symbols at the end of the paper.

Energy Balance

The second part of the model is the energy balance

$$\frac{dT_m}{dt} = aJ_{cris} + bF_f + cJ_{vap} + d \tag{4}$$

where a, b, c, d incorporate the enthalpy terms and specific heat capacities derived as functions of physical and thermodynamic properties, see [6].

Population Balance (in volume coordinates)

The kinetics mechanisms of nucleation, crystal growth and particle agglomeration are defined by the population balance. There are different mathematical representations of it depending on the crystallization phenomena taken into account. Most of the crystallizer models reported in the literature neglect the agglomeration effect. For the process in hand, this assumption appears to be irrelevant since agglomeration is registered in the process run. The population balance is expressed by the leading moments of CSD in volume coordinates since agglomeration must obey mass conservation law

$$\frac{d\tilde{\mu}_0}{dt} = \tilde{B}_0 \ -\frac{1}{2}\beta'\tilde{\mu}_0^2 \tag{5.1}$$

$$\frac{d\tilde{\mu}_1}{dt} = G_v\tilde{\mu}_0 \tag{5.2}$$

$$\frac{d\tilde{\mu}_2}{dt} = 2G_v\tilde{\mu}_1 + \beta'\tilde{\mu}_1^2 \tag{5.3}$$

$$\frac{d\tilde{\mu}_3}{dt} = 3G_v\tilde{\mu}_2 + 3\beta'\tilde{\mu}_1\tilde{\mu}_2 \tag{5.4}$$

with initial conditions $\tilde{\mu}_j(0) = 0, \quad j = 0,1,2,3.$

The main process nonlinearities are included in the crystallization rate

$$J_{cris} = \rho_c \frac{d\tilde{\mu}_1}{dt} \tag{6}$$

As for the kinetics parameters, nucleation rate ($\tilde{B}_0$), crystal growth rate (G) and agglomeration kernel (β'), it is difficult to formulate physically based mathematical models. Here, the empirical correlations have a long tradition and there exist in the literature a large number of empirical equations for the kinetics parameters [2,3]. The empirical descriptions considered here are extensively studied and reported in previous works [6]. Thus, the nucleation rate is defined as

$$\tilde{B}_0 = K_n \times 2.894 \times 10^{12} \ G^{0.51}\left(\frac{\tilde{\mu}_1}{k_v\ V_m}\right)^{0.53} V_m \tag{7}$$

the agglomeration kernel is

$$\beta' = K_{ag} G\left(\frac{\tilde{\mu}_1}{V_m^2}\right) \tag{8}$$

and the linear growth rate is

$$G = Kg\exp\left[-\frac{57000}{R(T_m{+}273)}\right](S-1) \times\exp\left[-13.863(1-P_{sol})\right]\left(1+2\frac{v}{V_m}\right) \tag{9}$$

from which the volume growth rate is determined

$$G_v = 3k_v^{1/3}\left(\frac{v}{\tilde{\mu}_0}\right)^{2/3} G \tag{10}$$

K_g, K_n and K_{ag} are tuning kinetic constants, optimised on the basis of the classical non-linear least-squares regression.

4 Data-based Model (Black Box Model)

Data based modeling techniques are methods that are able to extract process knowledge from measured data. The rapid growth of computational resources led to the development of a wide number of data based modeling techniques, the most common among which are artificial neural networks (ANNs). Their ability to approximate complex non-linear relationships without prior knowledge of the model structure makes them a very attractive alternative to classical modeling techniques [7].

The pure ANN approach is applied for modeling of the same industrial sugar crystallization process as defined in section 2. An obvious advantage of this approach is its universal character in approximating different physical phenomena with similar computational structures. It saves time and effort identifying parameters, in contrast to the case when an analytical model is developed. However, there are some remarkable disadvantages of the ANN modeling approach. First, it suffers from a lack of transparent structure and physical understanding of the network parameters. The resulting black-box (input-output) model in general does not provide the transparency required to understand the process. Secondly, it relies only on the recorded data and does not exploit any other source of knowledge available for the process at hand.

The choice of the network structure depends on the available process data, the desired model accuracy and the assumed model complexity. The ANN model of the sugar crystallization contains nine inputs and two outputs (see Fig. 2).

The inputs are related to on-line collected physical measurements of flowrate, brix, and temperature of the fed liquor/syrup, flowrate of water, flowrate, temperature and pressure of the steam, the pressure and temperature of the vacuum. The network outputs are the brix and temperature of the solution for which historical data are also available.

To improve the efficiency of network training pre-processing and post-processing techniques are provided. Before training the network inputs and targets are scaled so that they always fall into a certain range, [0.01,1] for the present network. All data points corresponding to each input and target are divided by the respective maximum value. After the training is over the network outputs are converted back into the original units.

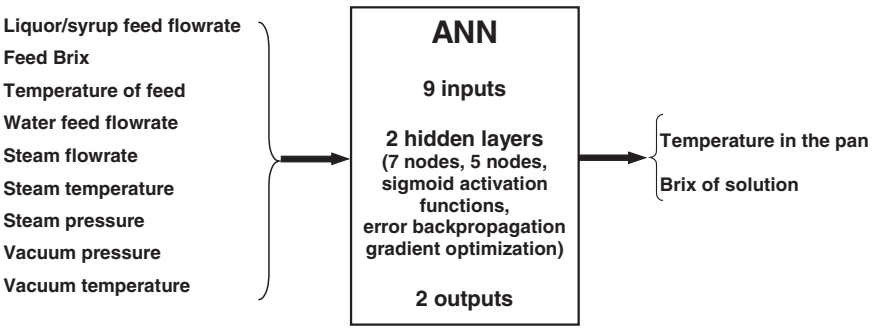

Figure 2. Data-driven model structure of sugar crystallization process.

5 Knowledge-based Hybrid Model (Grey Box Model)

Hybrid modeling provides an efficient alternative to the modeling techniques discussed in the previous sections and offers clear advantages compared to pure data-based modeling approaches [8,9]. The idea of hybrid modeling is to complement mechanistic models with the data-based approach. In the design of such models it is possible to combine theoretical and experimental knowledge, as well as process information from different sources: theoretical knowledge from physical and mass conservation laws; experimental data from pilot plant or industrial plant experiments; data from regular process operation; knowledge and experience from qualified process operators. A clear advantage of the hybrid NN is that less training data is required.

The third sugar crystallization model is a combination between an ANN and first principle equations in a serial hybrid structure, where the known physical constrains (the mass, energy and population balances) are modelled by their analytical expressions (Eqs. 1–6) and the kinetic parameters are approximated by an ANN (see Fig. 3).

The kinetic parameters are affected by the temperature (T_m), supersaturation (S), purity of the solution (Pur_{sol}) and volume fraction of crystals (υ_c). They all are considered as networks inputs. Except for temperature, the other inputs are not directly measured. They are inferred from estimated mass balance states [6] and together with the measurements are saved in a large database.

A typical problem arising by the hybrid network modeling is that the usual procedure for training do not work. At each step the neural network training requires the error between the network output and the corresponding target output. In the hybrid system, however, the target outputs are not available since the kinetic parameters are not measured. Hence, a new training procedure must be developed. The sensitivity approach proposed by [10] is applied for training of the present model. The network outputs are propagated through the analytical part of the model and the hybrid model output is compared with the available data. The mass of crystals is considered as most appropriate variable to serve as a target output in the hybrid network training (Fig. 4).

According to Eqs. (1.4), (5.2), (6), and (10), the mass balance of crystals can be rewritten as

$$\frac{dM_c^{hyb}}{dt} = 3(k_v \rho_c)^{1/3} (\tilde{\mu}_0^{hyb})^{1/3} (M_c^{hyb})^{2/3} G^{NN} \qquad (11)$$

Eq. (11) is incorporated in the hybrid training structure. Note that in order to integrate it the zeroth moment ($\tilde{\mu}_0$) is required. Therefore, its balance equation is also involved in the network training stage,

$$\frac{d\tilde{\mu}_0^{hyb}}{dt} = B^{NN} - \frac{1}{2}\beta^{NN}\left(\tilde{\mu}_0^{hyb}\right)^2 \qquad (12)$$

Superscripts *hyb* and *NN* are used to point out variables obtained during the hybrid network training. The network outputs give estimates of the growth rate, nucleation and agglomeration kinetic parameters. These estimates are propagated through (11,12). The error signal for updating the network parameters

$$e_{tr} = e_{obs}\left[\lambda_G \ \lambda_B \ \lambda_\beta\right]^T \qquad (13)$$

is obtained by multiplying the observed error ($e_{obs} = M_c^{data} - M_c^{hyb}$) with the gradient of the hybrid model output with respect to the network outputs

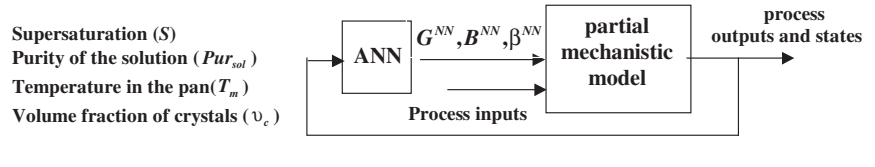

Figure 3. KBHM structure of sugar crystallization process.

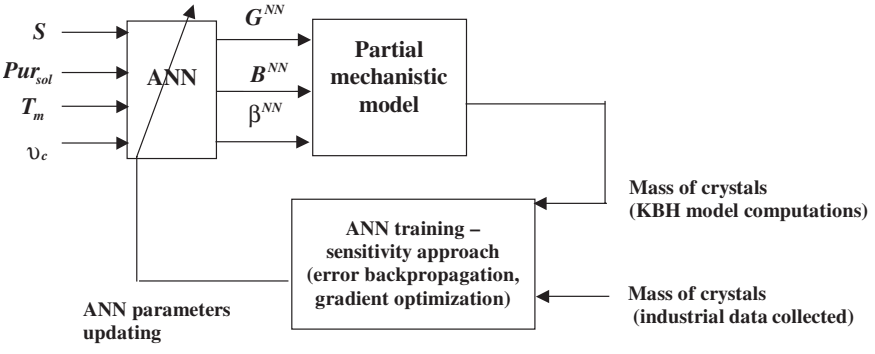

Figure 4. Hybrid ANN training structure.

$$\lambda_G = \frac{\partial M_c^{hyb}}{\partial G}, \lambda_B = \frac{\partial M_c^{hyb}}{\partial B}, \lambda_\beta = \frac{\partial M_c^{hyb}}{\partial \beta} \quad (14)$$

The gradients (14) can be computed through integration of the *sensitivity equations*

$$\frac{d\lambda_G}{dt} = \frac{\partial f_2}{\partial M_c^{hyb}}\lambda_B + \frac{\partial f_2}{\partial G}, \lambda_G(0) = 0 \quad (15.1)$$

$$\frac{d\lambda_B}{dt} = \frac{\partial f_2}{\partial M_c^{hyb}}\lambda_B + \frac{\partial f_2}{\partial \tilde{\mu}_0^{hyb}}\left(\frac{\partial \tilde{\mu}_0^{hyb}}{\partial B}\right), \lambda_B(0) = 0 \quad (15.2)$$

$$\frac{d\lambda_\beta}{dt} = \frac{\partial f_2}{\partial M_c^{hyb}}\lambda_\beta + \frac{\partial f_2}{\partial \tilde{\mu}_0^{hyb}}\frac{\partial \tilde{\mu}_0^{hyb}}{\partial \beta}, \lambda_\beta(0) = 0 \quad (15.3)$$

where f_2 is the right hand side of (11).

Note, that while λ_G can be straightforwardly obtained, λ_B and λ_β depend on the gradients of the zeroth moment with respect to B and β, respectively. Therefore, in order to determine λ_B and λ_β the same strategy is used leading to the integration of the following sensitivity equations with zero initial conditions

$$\frac{d\chi_B}{dt} = \frac{\partial f_1}{\partial \tilde{\mu}_0}\chi_B + \frac{\partial f_1}{\partial B}, \chi_B(0) = 0 \quad (16.1)$$

$$\frac{d\chi_\beta}{dt} = \frac{\partial f_1}{\partial \tilde{\mu}_0}\chi_\beta + \frac{\partial f_1}{\partial \beta}, \chi_\beta(0) = 0 \quad (16.2)$$

where $f_1 = B^{NN} - \frac{1}{2}\hat{\beta}^{NN}\left(\tilde{\mu}_0^{hyb}\right)^2$

$$\chi_B = \frac{\partial \tilde{\mu}_0}{\partial B}, \qquad \chi_\beta = \frac{\partial \tilde{\mu}_0}{\partial \beta} \quad (17)$$

6 White Box, Black Box and Grey Box Model Predictions versus Industrial Data

6.1 Process (Measured) Output Predictions

In this section the performance of the three models is examined with respect to prediction quality of the process outputs: temperature of massecuite (T_m) and brix of solution (Bx_{sol}). The time trajectories of T_m and Bx_{sol} are depicted on Figs. 5 and 6.

Fig. 5 shows the results of the training stage. Data are denoted by x-shaped lines, the dotted lines correspond to the predicted values by the mechanistic model, the dashed lines are ANN model predictions and by solid lines are depicted the same outputs computed by the hybrid model. The hybrid model (with 38 tuning parameters) was able to capture the process dynamics better than the mechanistic model (with 3 tuning parameters) and ANN model (with 44 parameters).

Fig. 6 depicts the results related to the generalisation properties of the three models. Once the training was over the network weights were frozen and tested on a new (validation) batch. Note, that the hybrid model clearly exhibited superior

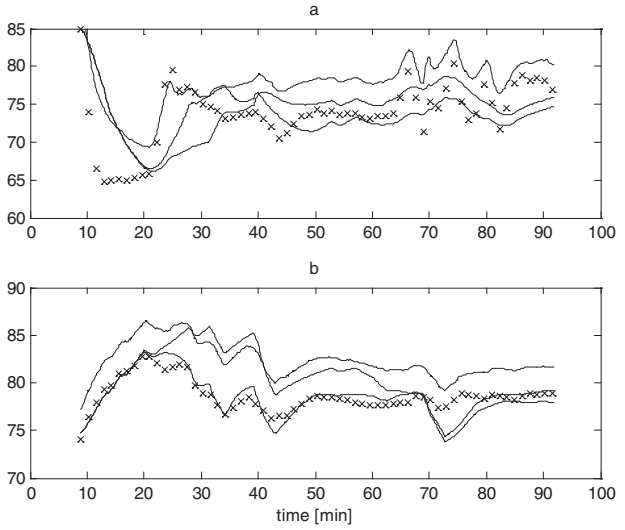

Figure 5. *Training stage.* Process output predictions by the hybrid model (solid line), the analytical model(doted line) and ANN model (dashed line) compared with industrial process data *(*x line).

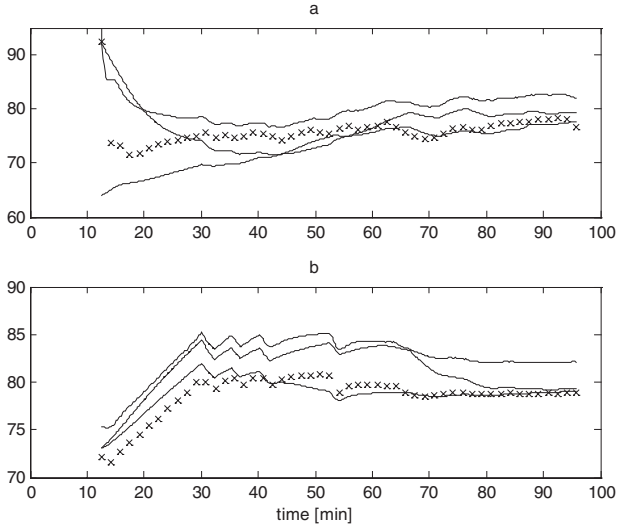

Figure 6. *Validation stage.* Process output predictions by the hybrid model (solid line), the analytical model (doted line) and ANN model (dashed line) compared with industrial process data (x line).

performance with respect to predictions of brix. As for temperature, even though the ANN model gave a bit worse approximates, globally the three models showed similar extrapolations, apart from the initial transient period (10–25 min.) before the temperature settled down. The physical interpretation behind this phenomenon is that temperature was not substantially affected by process dynamics and kinetic mechanisms, respectively.

6.2 CSD Predictions

The difficulty in modeling crystallization is essentially in the accurate description of the CSD with the respective quantities – MA and CV.

The quality of crystal size distribution is expressed at industrial level in terms of the norms approved by ICUMSA (International Commission for Uniform Methods of Sugar Analysis), i.e. by the mean size (MA) and by the coefficient of variation (CV) of the mass-size distribution function *m(L)*. There are no techniques for (on-line) direct measurement of such parameters and generally data are limited to measurements made at the end of each batch by laboratory (sieve) analysis. Thus, we need to know the moments of the mass-size distribution which are defined as

$$\eta_j(L) = \int_0^\infty L^j m(L) dL, j = 0, 1, 2, 3, ... \quad (18)$$

In order to account for the agglomeration mechanism we have the population balance expressed as number-volume distribution moments (Eq. (5)). Therefore, a relation between mass-size and number-volume moments is required. The recovering method adopted in this work is based on the assumption that the final sugar mass-size distribution can be reasonably well represented by a normal distribution function, which was confirmed by statistical data analysis presented in the next subsection.

The *j*th moment of a normal distribution for any type of particle distribution function, here applied to the mass-size distribution can be defined as a function of the mean ($\bar{L}$) and the variance (σ) of the distribution as follows:

$$\eta_j(L) = \sum_r \left[\left(2^{1/2}\sigma\right)^{j-r} (\overline{L})^r \frac{j!.1.3....(j-r-1)}{(j-r)!\ r!\ 2^{(j-r)/2}} \right] \quad (19)$$

where $r = 0,2,4$ ..., j for j even and $r = 1,3,5,$ ..., j for j odd. By definition

$$MA = \overline{L} \quad (20)$$

$$CV = \frac{\sigma}{\overline{L}} 100 \quad (21)$$

Hence, it is required to know only two moments of the mass size distribution in order to compute the mean and the variance. At this point it is relevant to recall basic relationships between crystal mass-size ($m(L)$), number-volume ($n(v)$) and number-size ($n(L)$)distribution functions [11],

$$\nu = k_\nu L^3 \quad (22)$$

$$n(L)dL = n(\nu)d\nu \quad (23)$$

$$m(L) = \rho_c k_v L^3 n(L)/M_c \quad (24)$$

where $M_c = \rho_c \mu_1(\nu)$ is the total crystal mass. With the aid of the above definitions, the relation between the mass-size ($\eta_j(L)$) and number volume ($\tilde{\mu}_j(\nu)$) moments is given by

$$\eta_j(L) = \frac{1}{M_c}\left(\frac{\rho_c}{k_v^{k-1}}\mu_k(\nu)\right), \quad k = \frac{j}{3} + 1,\ j = 0, 3, 6, ... \quad (25)$$

The model based estimation of the MA and CV goes through the following steps: i) For a given set of number-volume moments $\tilde{\mu}_k(\nu)$, obtained by the model (5), $\eta_3(L)$ and $\eta_6(L)$ mass-size moments are obtained from (25); ii) $\overline{L}$ and σ are computed from (19) for $j = 3,6$. iii) The CSD is evaluated by (20) and (21).

Following the above procedure, MA and CV predicted by the first principles model and the KBHM, are compared with the experimental data available at the end of a batch.

The results of 14 (validation) batches are summarised in Tab. 3. The average errors demonstrate a better agreement between experimental data and hybrid model predictions than that observed with the complete mechanistic model.

Table 3. Final CSD – Experimental data versus hybrid and mechanistic model predictions.

batch No.	experimental data		hybrid model		mechanistic model	
	MA [mm]	CV [%]	MA [mm]	CV [%]	MA [mm]	CV [%]
1	0.479	32.6	0.518	28.12	0.583	21.26
2	0.559	33.7	0.491	29.34	0.542	18.43
3	0.680	43.6	0.575	32.65	0.547	18.69
4	0.494	33.7	0.514	35.16	0.481	14.16
5	0.537	32.5	0.599	29.52	0.623	24.36
6	0.556	35.5	0.496	28.49	0.471	13.642
7	0.560	31.6	0.658	35.67	0.755	34.9
8	0.530	31.2	0.609	36.87	0.681	27.39
9	0.485	47.2	0.501	38.4	0.466	34.1
10	0.549	44.0	0.517	38.9	0.453	34.3
11	0.527	39.3	0.489	37.2	0.466	34.9
12	0.547	39.1	0.496	40.2	0.418	36.1
13	0.512	32.7	0.487	29.9	0.402	36.4
14	0.568	41.2	0.519	39.2	0.441	34.5
av. error			**7.8%**	**13.4%**	**13.7%**	**36.1%**

6.3 Statistical Comparison of the Significance of Predicted Values of MA and CV between the Hybrid and Mechanistic Model

Single factor analysis of variance (ANOVA) were conducted using the statistical program R [12] to examine the ability of the hybrid model and the mechanistic model in accurately predicting experimental data values for MA and CV. Each ANOVA model consisted of a response term (MA or CV) and a single model term with 3 different levels, i.e. experimental data (level 1), predicted values from the hybrid model (level 2), and the predicted values from the mechanistic model (level 3). Standard regression diagnostic methods were subsequently used to assess the reliability of these ANOVA models to the assumption of normality, in the identification of outliers and the examination of influencial cases on estimated regression parameters [13].

A multiple comparison test using Tukey's honestly significant difference method, was conducted to compare the differences between the average values from the experimental data, the hybrid model and the mechanistic model, when the

null hypothesis of equality between the mean values of the 3 different groups of data were rejected by the analysis of variance at a 5 % level of significance.

The analysis of variance showed that there was no significant difference (p-value = 0.8079) between the predicted values of MA by the hybrid model and the mechanistic model, to that of the experimental data (Tab. 3). Essentially, both models predicted the experimental data of MA equally well. However, the analysis of variance showed that not all of the mean values for CV between the three groups of data (the experimental data, the predicted values from the hybrid model and the predicted values of the mechanistic model) were similar (p-value = 0.0009). Tukey's honestly significant difference (p-value < 0.05) showed that only the hybrid model could give reliable predictions of CV, whereas the mechanistic model gave significantly different predicted values (see Fig. 7).

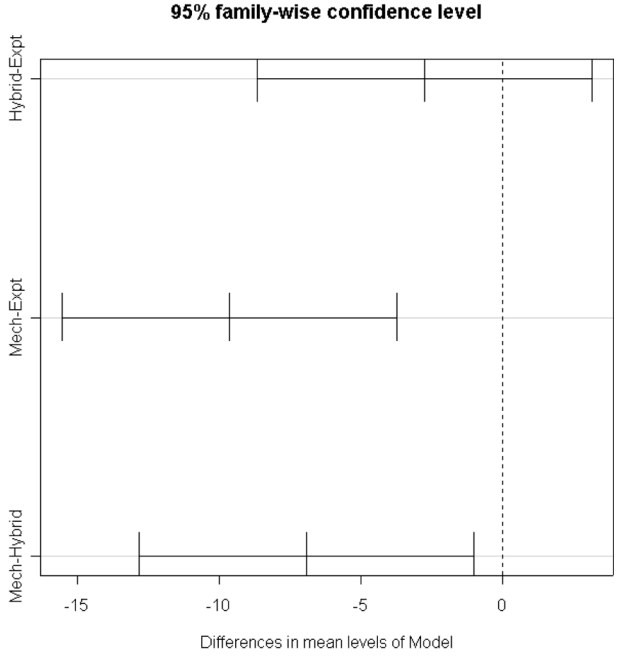

Figure 7. Plot of the differences in the average CV values and their 95 % confidence intervals, calculated from Tukey's Honestly significant difference test, for the coefficient of variation between (i) predicted values from hybrid model with experimental data (Hybrid-Expt), (ii) predicted values from mechanistic model with experimental data (Mech-Expt), (iii) predicted values from hybrid model with predicted values from mechanistic model (Hybrid-Mech).

7 Conclusions

In this paper three approaches for modeling of a sugar crystallization process were comparatively investigated. They are termed *white box models*, which express physical knowledge by means of mathematical equations, *black box models*, those that are able to extract information only from process data and *grey box models,* also known as knowledge based hybrid models (KBHM), which are a logical combination of the aforementioned models.

The KBHM offers a reasonable compromise between the extensive efforts in obtaining a fully parameterised structure, as with mechanistic models and the poor generalisation of the complete data-based modeling approaches. We have demonstrated that the KBHM of the crystallization process considered in this study compares well with the experimental data and in fact is the best process model.

However, it is fair to say that hybrid models also have their disadvantages. They are considerably complex, require sophisticated software tools and computation power, although the later is becoming of a less problem. The lack of theoretical generalisation of the existing problem dependent solutions is to be considered more as a scientific challenge in this area than as a disadvantage. Still more research work has to be done on analysing the level of compatibility and more efficient combinations between different knowledge sources.

On the basis of this case study it can be concluded that if a reliable first principles model exists it is recommendable to use it. Otherwise, a practically more sound approach is to build a model that retains the advantages of both analytical and data based methodologies, i.e. hybrid modeling.

Acknowledgements

Petia Georgieva is on leave from the *Institute of Control and System Research, Bulgarian Academy of Sciences, Bulgaria*, supported by EU RTN Project BatchPro HPRN-CT-2000-00039. This work was further financed by the Portuguese Foundation for Science and Technology within the activity of the Research Unit *Institute for Systems and Robotics-Porto.*

Received: December 19, 2002 [CET 1768]

Symbols used

B_0	[1/m^3 s]	nucleation rate
BPE	[°C]	Boiling Point Elevation
B	[–]	Brix (mass fraction of dissolved solids)
CV	[%]	coefficient of variation
F	[m^3/s]	feed flowrate
F_s	[kg/s]	steam flowrate
G	[m/s]	linear growth rate
G_v	[m^3/s]	overall crystal volume growth rate
K_{ag}	[–]	crystal agglomeration kinetic constant
K_g	[–]	crystal growth kinetic constant
K_n	[–]	crystal nucleation kinetic constant
k_v	[–]	volume shape factor
k_{vap}	[–]	parameter of the evaporation rate (Eq. (3))
L, $\overline{L}$	[–]	particle size; mean size of a population distribution
m(L)	[1/m]	crystal mass-size distribution function
M	[kg]	mass
MA	[m]	mass averaged crystal size
n(v)	[1/m^6]	crystal number-volume distribution function

$n(L)$	[1/m^4]	crystal number-size distribution function
Pur	[–]	purity (mass fraction of sucrose in the dissolved solids
Q	[J/s]	heat input
R	[J/molK]	gas constant
S	[–]	supersaturation
t	[s]	time
T	[°C]	temperature
v	[m^3]	crystal volume
V	[m^3]	volume
W	[J/s]	stirring power

Greek symbols

α_s	[–]	parameter of the heat input (Eq. (2))
β	[m^3/s]	agglomeration kernel
β'	[1/s]	agglomeration kernel at any time for vessel volume
$\lambda_{w(vac)}$	[J/kg]	latent heat of water evaporation
$\tilde{\mu}_j(v)$	[m^{3j}/(m^3)]	j-moment of number-volume distribution function $n(v)$
$\eta_j(L)$	[m^j]	j-moment of mass-size distribution function $m(L)$
ρ	[kg/m^3]	density
σ	[–]	variance of a population distribution
υ_c	[–]	volume fraction of crystals

Subscripts

c	crystals
cris	crystallization
f	feed
i	impurities
m	massecuite
s	sucrose
sat	saturation
seed	seeding
sol	solution
syr	syrup
vac	vacuum
vap	evaporation
w	water

Superscripts

hyb	hybrid
NN	Neural Network
~	based on total vessel volume, ($\tilde{x} = xV_m$)

References

[1] S. Feyo de Azevedo, B. Dahm, F. R. Oliveira, *Comput. Chem. Eng.* **1997**, *21*, S751.

[2] S. Chorão, S. Feyo de Azevedo, A Discretized Population Balance Approach for the Modeling of Industrial Sucrose Crystallization, *Proc. of 13th Symp. on Industrial Crystallization*, Toulouse, France, 16–19 September, **1996**, 719.

[3] P. Lauret, H. Boyer, J. C. Gatina, *Control Eng. Practice*, **2000**, *8*, 299.

[4] M. J. G. Meireles, S. Feyo de Azevedo, Modeling the Operation of a Sugar Industrial Evaporative Crystallizer, *Proc. Of Chempor';98*, Lisbon, Portugal, 26–28 September, **1998**, 807.

[5] K. Najim, V. Ruiz, S. Feyo de Azevedo, M.J. Goncalves, *J. Systems Eng.* **1996**, *6*, 233.

[6] S. Feyo de Azevedo, J. Chorão, M. J. Gonçalves, L. Bento, *Int. Sugar J.* **1994**, *96*, 18.

[7] L. Chen, O. Bernard, G. Bastin, P. Angelov, *Control Eng. Practice* **2000**, *8*, 821.

[8] J. Schubert, R. Simutis, M. Dors, I. Havlik, A. Lubbert, *J. Biotechnol.* **1994**, *35*, 51.

[9] J. Graefe, P. Bogaerts, J. Castillo, M. Cherlet, J. Werenne, P. Marenbach, R. Hanus, *Bioprocess Eng.* **1999**, *21*, 423.

[10] D. C. Psichogios, L. H. Ungar, *AIChE J.* **1992**, *38 (10)*, 1499.

[11] A. D. Randolph, M. A. Larson, *Theory of Particulate Processes – Analyses and Techniques of Continuous Crystallization*, Academic Press, Cambridge **1988**.

[12] R. Ihaka, R. Gentleman, *J. Comput. Graphical Statistics* **1996**, *5*, 299.

[13] J. Neter, M. H. Kutner, C. J. Nachtshem, W. Wasserman, *Applied Linear Statistical Models*, ■Publisher?■ Irwin, USA, 1996.

